

X-Ray Absorption Spectroscopy and Computer Modelling Study of Nanocrystalline Binary Alkaline Earth Fluorides

This content has been downloaded from IOPscience. Please scroll down to see the full text.

2015 IOP Conf. Ser.: Mater. Sci. Eng. 80 012005

(<http://iopscience.iop.org/1757-899X/80/1/012005>)

View [the table of contents for this issue](#), or go to the [journal homepage](#) for more

Download details:

IP Address: 194.95.157.141

This content was downloaded on 08/08/2016 at 12:22

Please note that [terms and conditions apply](#).

X-Ray Absorption Spectroscopy and Computer Modelling Study of Nanocrystalline Binary Alkaline Earth Fluorides

A.V. Chadwick¹, A. Düvel², P. Heitjans², D.M. Pickup¹, S. Ramos¹, D.C. Sayle¹ and T.X.T. Sayle¹

1 School of Physical Sciences, University of Kent, Canterbury, Kent CT2 7NH

2 Institute of Physical Chemistry and Electrochemistry, Gottfried Wilhelm Leibniz University Hannover, Callinstrasse 3a, D-30167 Hannover, Germany

E-mail: a.v.chadwick@kent.ac.uk

Abstract. Nanocrystalline samples of $\text{Ba}_{1-x}\text{Ca}_x\text{F}_2$ prepared by high-energy milling show an unusually high F^- ion conductivity, which exhibit a maximum in the magnitude and a minimum in the activation energy at $x = 0.5$. Here, we report an X-ray absorption spectroscopy (XAS) at the Ca and Sr K edges and the Ba L_3 edge and a molecular dynamics (MD) simulation study of the pure and mixed fluorides. The XAS measurements on the pure binary fluorides, CaF_2 , SrF_2 and BaF_2 show that high-energy ball-milling produces very little amorphous material, in contrast to the results for ball milled oxides. XAS measurements of $\text{Ba}_{1-x}\text{Ca}_x\text{F}_2$ reveal that for $0 < x < 1$ there is considerable disorder in the local environments of the cations which is highest for $x = 0.5$. Hence the maximum in the conductivity corresponds to the composition with the maximum level of local disorder. The MD calculations also show a highly disordered structure consistent with the XAS results and similarly showing maximum disorder at $x = 0.5$.

1. Introduction

There are numerous reports in the literature that atomic migration in nanocrystals is unusually fast compared to the parent bulk. In ionic materials the origin for enhanced diffusion has been assigned to atomic disorder along interfaces and surfaces [1-4], however, in many cases, the experimental data in many cases are ambiguous. The data for the binary oxides is particularly varied and is very dependent on the method of sample preparation [5-9]. In contrast unusually high ionic conductivities have been established in nanocrystalline alkaline earth fluorides. Conductivity measurements on pressed pellets of 9 nm particles of calcium fluoride prepared by the inert gas condensation method showed values approximately four orders of magnitude higher than bulk material [10] and were interpreted in terms of the space charge model [11] developed by Maier [12-14]. The space charge model was also used to interpret the exceptionally high ionic conductivity of barium fluoride (BaF_2) [15]. This work was followed by a report by Heitjans and co-workers of high fluoride ion diffusivity in high-energy ball-milled nanocrystalline BaF_2 and CaF_2 as well as in BaF_2 - CaF_2 composites [16]. Later work [17] revealed that nanocrystalline high-energy ball-milled BaF_2 and CaF_2 had a conductivity two orders of magnitude higher than the parent compounds. In addition, the



presence of a metastable ternary $\text{Ba}_{1-x}\text{Ca}_x\text{F}_2$ compound which retained the cubic fluorite structure was detected [17]. It was shown that this compound could be prepared in nanocrystalline form for $0 \leq x \leq 1$ by high-energy ball-milling and the conductivity had a well-defined maximum at $x = 0.5$ and a minimum in the activation energy at the same composition [18]. In addition, high speed magic angle spinning (MAS) ^{19}F NMR revealed that there were five distinct F^- sites [18]. These sites are characterized by a distinct number of Ba and Ca cations in the first coordination shell: $[\text{Ba}]_n[\text{Ca}]_{4-n}$ ($0 \leq n \leq 4$). The mixed sites with $n = 1, 2, 3$ dominate the NMR spectra at intermediate values of x . Presumably, the mixed cation sub-lattice causes the metastability of the compounds, influences both the formation energy of, for example, F^- interstitials for example, as well as their migration energy leading to the observed fast ion conduction. A molecular dynamics simulation of the system [19] rationalised the effects as due to the large size difference between the cations, with Ca^{2+} favouring the formation of nearest neighbour interstitial F^- ions and Ba^{2+} favouring the formation of neighbouring F^- vacancies.

In this contribution we report the results of X-ray absorption spectroscopy (XAS) measurements and molecular dynamics (MD) simulation studies of $\text{Ba}_{1-x}\text{Ca}_x\text{F}_2$. These probe the local structure and provide insight into the origins of the conductivity behavior.

2. Methodology

2.1 Materials

High energy ball-milling was used to prepare nanocrystalline CaF_2 , SrF_2 , BaF_2 , $\text{Ba}_{1-x}\text{Ca}_x\text{F}_2$ ($x = 0, 0.25, 0.5, 0.75$ and 1), $\text{Ca}_{0.5}\text{Sr}_{0.5}\text{F}_2$ and $\text{Ba}_{0.5}\text{Sr}_{0.5}\text{F}_2$ using procedures described in reference [18]. The particles sizes as determined from the broadening of the peaks in the XRD powder patterns were typically 9-13 nm, if calculated with the Scherrer equation or 30-60 nm if the Williamson and Hall equation was used to include strain broadening. For the XAS measurements the powders were mixed with cellulose diluent and pressed into 13 mm diameter pellets.

2.2 XAS measurements

XAS scans were collected for the appropriate edge (Ca and Sr K edges, Ba L_3 edge) at room temperature on beam line B18 at the Diamond Light Source [20]. Data collection used transmission mode with ion chamber detectors. Continuous scanning (QEXAFS) was employed; an individual scan required 180 s and several scans were performed to improve the signal-to-noise ratio. The synchrotron energy and current were 3 GeV and 300 mA, respectively. The beam size at the sample was 700×700 microns. Powdered samples were mixed with cellulose as a diluent and pressed into 13 mm diameter pellets. The spectra were normalized in Athena and fitted to scattering models in R-space produced by FEFF in Artemis [21].

2.3 Molecular dynamics simulation

MD simulations were performed using the DL-POLY code [22]. The Born model of the ionic solid, together with full ionic charges, was used to describe the Ba-F, Ca-F and F-F interactions. The nanoparticles, which comprised 13824 anions and 6912 metal cations, were generated using simulated amorphisation and recrystallisation [23]; three model nanoparticle solid solutions were generated: $\text{Ba}_{0.25}\text{Ca}_{0.75}\text{F}_2$, $\text{Ba}_{0.5}\text{Ca}_{0.5}\text{F}_2$ and $\text{Ba}_{0.75}\text{Ca}_{0.25}\text{F}_2$.

3 Results and discussion

3.1 XAS measurements

All the spectra were analysed to yield the details of the local structure, i.e. bond lengths, Debye-Waller factors, etc., however the qualitative information is best represented by the Fourier transform (FT) of the k^3 weighted normalised EXAFS and these will be used in this short paper. Firstly, we consider the FTs of nanocrystalline and bulk CaF_2 shown in Figure 1. Very similar results were found for SrF_2 and BaF_2 (not shown here). There is very slight attenuation of the peaks in the nanocrystalline material, which is a distinct contrast to the XAS data for ball-milled oxides [5, 6, 24]. This indicates that the high-energy ball-milled binary fluorides are highly ordered with minimal amounts of amorphous material, possibly due to stronger ionic bonding in the fluorides. It seems reasonable to assume the high-energy ball-milled ternary $\text{Ba}_{1-x}\text{Ca}_x\text{F}_2$ compound has a similar low amorphous content.

The FTs of the Ca K edge EXAFS of the $\text{Ba}_{1-x}\text{Ca}_x\text{F}_2$ samples are shown in Figure 2. The two dominant peaks in the plot at ~ 2.3 Å and ~ 3.8 Å correspond to the nearest neighbor shell of eight F⁻ ions and the shell of next-nearest neighbour cations, respectively. These peaks are clearly attenuated for the samples with $x < 1$ as a result of the disorder created in the local structure due to the replacement of Ca^{2+} by the larger Ba^{2+} cation. The effect is greatest for $x = 0.5$, where the second peak has almost disappeared, showing this sample has the highest level of disorder. Similarly the Ba L₃ edge EXAFS of these samples showed that the FT was most attenuated for the sample with $x = 0.5$. The maximum observed in the conductivity of this system is also found at $x = 0.5$ [18] and it is reasonable to associate this with the maximum level of local disorder.

3.2 MD simulations

Analysis of the model nanoparticles revealed all three $\text{Ba}_{1-x}\text{Ca}_x\text{F}_2$ samples ($x = 0.25$, $x = 0.5$ and $x = 0.75$) were crystalline and conform to the fluorite crystal structure. The particles were highly disordered with F⁻ anions located far from their lattice sites; domains rich in either Ca or Ba showed relatively less disorder of the local anion sub-lattice compared to domains comprising Ca and Ba on neighbouring cation sites.

The nanoparticle with $x = 0.5$ comprised the highest level of sub-lattice disorder, Figure 3, in accord with the EXAFS data. There is a higher probability of finding Ca and Ba ions on

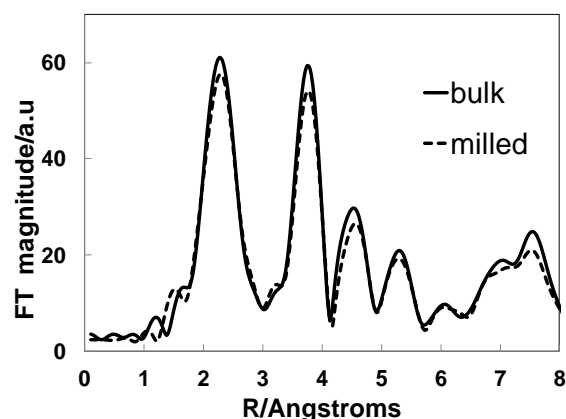


Figure 1. The FT of the normalised Ca K edge EXAFS of CaF_2 .

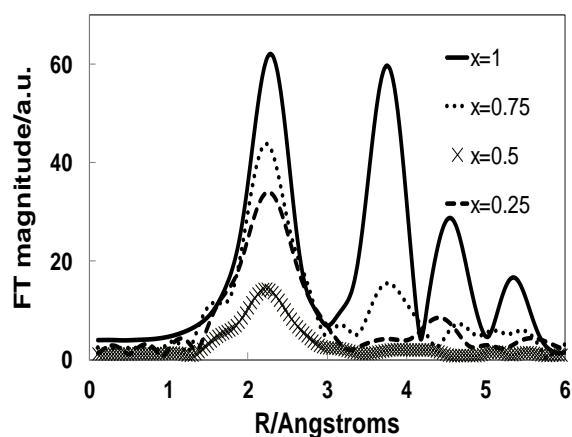


Figure 2. The FT of the normalised Ca K edge EXAFS of $\text{Ba}_{1-x}\text{Ca}_x\text{F}_2$.

neighbouring lattice sites for the $x = 0.5$ system, compared to either the $x = 0.25$ or $x = 0.75$ system, and therefore a higher probability of a disordered anion sub-lattice. The maximum disorder in the anion sub-lattice, at $x = 0.5$, coincides with the maximum in the conductivity. Accordingly, we attribute the high ionic conductivity to the disorder of the anion sub-lattice.

4. Conclusions

The important outcomes of this combined XAS and MD study are as follows:-

1. High-energy ball-milled CaF_2 , SrF_2 and BaF_2 contain very small amounts of amorphous material.
2. $\text{Ba}_{1-x}\text{Ca}_x\text{F}_2$ for $1 > x > 0$ is disordered with the maximum disorder at $x = 0.5$, which is the composition of the maximum ionic conductivity.

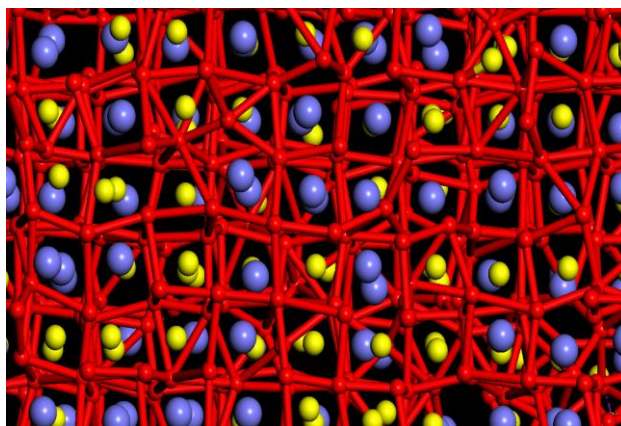


Figure 3. Ball and stick model of a segment of the $\text{Ba}_{0.5}\text{Ca}_{0.5}\text{F}_2$ nanoparticle showing the considerable disorder of the F^- anion sub-lattice. Ba^{2+} ions are coloured blue, Ca^{2+} ions are yellow and F^- ions are red. The sticks, linking the F^- ions, are included to help visualize the fluorite crystal structure.

References

- [1] Tuller H 2000 *Solid State Ionics* **131** 143
- [2] Indris S, Heitjans P, Roman H E and Bunde A 2000 *Phys. Rev.Lett.* **84** 2889
- [3] Guo X, Tan C and Yuan R-Z 1995 *J. Eur. Ceram. Soc.* **15** 25
- [4] Heitjans P and Indris S 2003 *J. Phys.: Condens. Matter* **15** 1257
- [5] Chadwick A V and Savin S L P 2009 *Solid State Electrochemistry I*, ed. V V Kharton (Weinheim: VCH-Wiley) p 79
- [6] Chadwick A V and Savin S L P 2010 *Low Dimensional Solids*, ed. D W Bruce, D O'Hare and R I Walton V V Kharton (Chichester: Weinheim: Wiley) p 1
- [7] Aydin H, Korte C and Janek J 2013 *Sci. Technol. Adv. Mater.* **14** 035007
- [8] Gerstl M, Frömling T, Schintlmeister A, Hutter H and Fleig J 2011 *Solid State Ionics* **184** 23
- [9] Schichtel N, et al J 2010 *Phys. Chem. Chem. Phys.* **12** 14596
- [10] Puin W and Heitjans P 1995 *Nanostruct. Mater.* **6** 885
- [11] Puin W, Rodewald S, Ramlau R, Heitjans P and Maier J 2000 *Solid State Ionics* **131** 159
- [12] Maier J 1987 *J. Electrochem. Soc.* **134** 1524
- [13] Maier J, Prill S and Reichert B 1988 *Solid State Ionics* **28–30** 1465
- [14] Maier J 1995 *Prog. Solid State Chem.* **23** 171
- [15] Sata N, Eberman K, Eber K and Maier J 2000 *Nature* **408** 946
- [16] Ruprecht B, Wilkening M, Steuernagel S and Heitjans P 2008 *J. Mater. Chem.* **18** 5412
- [17] Ruprecht B, Wilkening M, Feldhoff A, Steuernagel S and Heitjans P 2009 *Phys. Chem. Chem. Phys.* **11** 3071
- [18] Düvel A, Ruprecht B, Heitjans P and Wilkening M 2011 *J. Phys. Chem. C* **115** 23784
- [19] Zahn D, Heitjans P Maier J *Chem. Eur. J.* 2012 **18** 6225
- [20] Dent A J, et al 2013 *Journal of Physics: Conference Series* **430** 0120231
- [21] Ravel B and Newville M 2005 *J. Synchrot. Radiat.* **12** 537
- [22] Smith W and Forester T R 1996 *J. Mol. Graphics* **14** 136
- [23] Sayle D C, Mangili B C, Price D W and Sayle T X 2010 *Phys. Chem. Chem. Phys.* **12** 8584
- [24] Chadwick A V, et al 2003 *J. Phys.: Condens. Matter* **15** 431